W-TUBE ENERGY PILE HEAT TRANSFER MODEL WITH VARIABLE HEAT FLOW CONSIDERING HEAT EXCHANGE BETWEEN PILE AND CIRCULATING WATER

Shenglin Xi[a], Gang Shi[a*], Zhongming Wu[a] and Zijun Wei[a]

[a]School of Civil Engineering, Zhengzhou University, Zhengzhou 450001, P.R. China

In order to provide a more comprehensive depiction of the actual heat transfer process in energy piles, this research paper presents an approximate solution for a finite line heat source model operating under variable heat flow conditions. This solution is established by integrating the finite line heat source model and the superposition principle. Furthermore, the W-tube heat exchanger is divided into many segments, and a segmented superposition approach is used based on the thermal response. Consequently, a heat transfer model for a single-pile heat source is formulated, taking into consideration the heat exchange between the circulating water and the energy pile. Notably, the soil temperature predicted by this proposed model closely aligns with the results obtained from the FLUENT numerical model, thereby substantiating the accuracy of the proposed approach. Simultaneously, the heat transfer model is employed to analyze variations in temperature and heat flux density within the heat exchanger and to investigate the influence of parameters such as mass flow rate, pile-soil heat transfer coefficient, pile-soil density, and pile-soil specific heat capacity on the heat transfer characteristics of energy piles. This model enables the determination of time-varying heat flux and precise outlet temperature, thereby facilitating a rapid assessment of the heat transfer efficiency of energy piles.

Keywords: *energy pile; heat transfer model; variable source; section superposition method; heat transfer efficiency*

1. Introduction

The ground-source heat pump system has been widely used in building cooling and heating due to its energy-saving and environmental-protection characteristics, which are important for green buildings [1-3]. Traditional ground-source heat pump technology has a low heat exchange efficiency, high cost, and requires a wide area. To overcome these, a novel vertical buried-pipe ground-source heat pump system for an energy pile is required. Energy pile and building pile foundation synchronous construction share a relatively short construction duration; do not require an outdoor underground space; have a high heat transfer efficiency, high stability, and good durability，and offer economic benefits[1].

Establishing a heat transfer model for energy piles has been the focus at home and abroad, which is relevant for the engineering design and optimization of energy piles[4-6]. Classical analytical models typically rely on Kelvin's line source theory and cylindrical source model[7]. Based on the former, Ingersoll et al[8] established a vertical buried-tube heat exchanger model, which is the most widely used and mature heat transfer model. Applying the linear superposition principle, Green's

function method, and the virtual heat-source method, Zeng et al.[9] obtained the analytical solution for a finite linear heat source, which can describe the short-term unsteady heat-transfer characteristics of the ground heat exchanger well. Kavanaugh[10] regarded the vertically buried pipe heat exchanger as a cylindrical heat source, thus establishing a cylindrical heat-source model. Notably Cui et al.[13] proposed equidistantly dividing the helical tube into an annular heat source, established a transient annular heat-source model, and obtained the explicit analytical solution to the temperature response by using Green's function theory and the pixel method. Based on the theory of an infinite linear heat source, Yang et al.[14] and Ang et al.[15] considered the energy loss of circulating water and obtained the variable heat flow linear heat source model of the ground heat exchanger and its analytical solution. Akrouch et al.[16] established a new model based on the infinitely long hollow cylinder heat source model. This model assumes that the heat transfer between the entire heat exchanger tube and the surrounding soil is equal everywhere and reaches equilibrium at a specific time. Thus, the heat exchange per unit length (heat flux) was calculated. These analysis models are based on ideal simplifications, which include the medium being uniform. However, they cannot describe the heat transfer problem of energy piles in complex situations.

To consider the abovementioned problem, Li et al.[17,18] regarded the inlet and outlet branches of U-tubes as two infinite linear heat sources in the composite medium and established an infinite composite medium linear heat source model. This model is suitable for predicting the short-term heat transfer problem of underground heat exchangers. Li et al.[19] gave several analytical solutions to the heat conduction problems of linear, spiral, and cylindrical heat sources in infinite or semi-infinite anisotropic media based on point source theory. These analytical solutions provide a reference for analyzing the heat conduction of infinite or semi-infinite anisotropic materials with various heat sources. Luo et al.[20] proposed a new model for analyzing U-tube ground heat exchangers, which converts the simple and effective treatment method used for multilayer soil heat transfer into a composite-medium method for application to underground heat exchangers. This model is established by combining the treatment method of nonuniform wall temperature and the analysis model of unsteady ground-heat-transfer underground action. You et al.[21] developed an analytical model for helical coil energy group piles under seepage conditions by considering different heat flow densities of piles and the variation of heat flow density with time. Bezyan et al.[22] used FLUENT software to simulate the heat transfer rate and temperature distribution in the pile foundations of U-type, W-type, and spiral heat exchangers. Notably, few theoretical models of W-type buried-pipe energy piles and the heat transfer of energy piles under variable heat flux conditions exist. Therefore, to better describe the actual heat transfer process of energy piles, it is necessary to study the heat transfer of W-type buried-pipe energy piles under variable heat flux conditions.

Accordingly, an approximate solution of the finite linear heat source model under variable heat source conditions is proposed based on the finite linear heat source model and superposition principle. On this basis, the W-type heat exchanger is divided into multiple segments. The segmented heat flux–water temperature equations of the energy pile heat exchanger at different times are derived according to the heat transfer between the circulating water, and the energy pile and energy loss along the circulating water by leveraging the segmented superposition concept of the thermal response. Finally, the segmented-superposition heat-transfer model for a variable heat source of a single energy pile is established. This model can obtain the change in heat flux density with time and accurately

determine outlet temperature, which is convenient for rapidly evaluating the heat transfer efficiency of energy piles.

2. Approximate solution of finite linear heat source model of energy pile under variable heat source condition

During actual operation, the hourly change in building load leads to a dynamic change in heat exchange between the energy pile and soil. The constant-heat-source model has severe limitations, making it difficult to determine the specific-heat-source value. Therefore, a more accurate finite linear-heat-source model is needed for the analysis of long-term operation under variable heat-source conditions.

2.1. Finite linear-heat-source model

To calculate the heat transfer efficiency of a W-type buried-pipe energy pile, each heat exchange tube is usually regarded as a finite linear heat source. To obtain the analytical solution of the finite linear heat source, Zeng et al.[9] made the following assumptions:

(1) The thermophysical parameters of a semi-infinite space do not change with temperature.

(2) A semi-infinite space has a uniform initial temperature T_0.

(3) The surface temperature of a semi-infinite space remains unchanged during heat transfer.

(4) The linear heat source extends from the surface of the semi-infinite space to a certain depth *H*, and the heat flux per unit length q_l acts from $t = 0$ and is a constant.

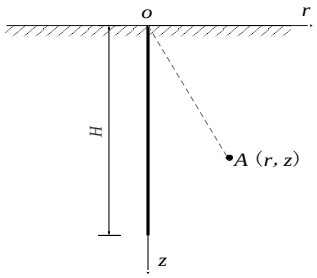

Figure 1 Finite linear heat source in a semi-infinite space

For a virtual heat source and under the superposition principle, the excess temperature at any point in the half-space caused by a finite linear heat source is

$$\theta(r,z,\tau)=\frac{q_l}{4\lambda\pi}\int_0^H\left\{\frac{erfc\left(\frac{\sqrt{r^2+(z-h)^2}}{2\sqrt{a\tau}}\right)}{\sqrt{r^2+(z-h)^2}}-\frac{erfc\left(\frac{\sqrt{r^2+(z+h)^2}}{2\sqrt{a\tau}}\right)}{\sqrt{r^2+(z+h)^2}}\right\}\mathrm{d}h \tag{1}$$

where r and z are the radials and vertical coordinates of any point A, respectively; $a=\lambda/\rho c$; a is the thermal diffusivity ($m^2 \cdot s^{-1}$) of the half-space medium; λ is the thermal conductivity ($W \cdot m^{-1} \cdot K^{-1}$) of the half-space medium; ρ is the density ($kg \cdot m^{-3}$); and c is the specific heat capacity ($J \cdot kg^{-1} \cdot K^{-1}$).

2.2. Thermal response approximate solution for finite linear heat source under variable heat source

During actual energy pile operation, the inlet temperature of the heat exchange tube can usually be regarded as having a constant value T_{in}. With the increase or decrease in energy pile temperature, the temperature difference between the circulating water in the heat exchange pipe and the surrounding pile gradually decreases, and the heat exchange efficiency decreases. Therefore, q_l is a time-varying variable $q_l(t)$.

To consider the change in heat source with time, $q_l(t)$ can be simplified as a q_l^k series with equal time interval$\Delta\tau$, as shown in fig.2(a), with $k = 1-N$. Therefore, the excess temperature of any point $A(r,z)$ in the semi-infinite space at time $N\Delta\tau$ under the action of heat flux $q_l(t)$ is presumably caused by a series of equal time intervals q_l^k, as shown in fig.2(a).

To calculate the excess temperature of any point A at moment $N\Delta\tau$, the heat flux density q_l^k in the period $(k-1)\,\Delta\,\tau\sim k\,\Delta$ is considered as an example. According to the superposition principle, the heat flux density q_l^k in this period can be regarded as the superposition of q_l^k that takes effect at moment $k\,\Delta\,\tau$ and heat flux density of -q_l^k, as shown in fig.2(b).

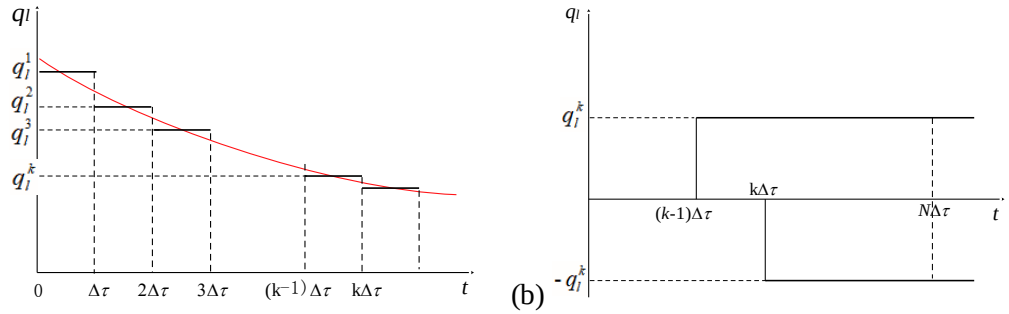

Figure 2. (a) Simplification of change in heat flux density $q_l(t)$ with time, (b) Superposition diagram of heat flux density q_l^k from period $(k-1)\,\Delta\,\tau$ to $k\,\Delta\,\tau$

According to the superposition principle, the excess temperature of point A caused by $(k-1)\,\Delta\,\tau\sim k\,\Delta\,\tau$ acting at time $N\,\Delta\,\tau$ can be expressed as

$$\theta^k\left(r,z,N\Delta\tau\right)=q_l^k\left[\Theta((N-k+1)\Delta\tau)-\Theta((N-k)\Delta\tau)\right]=q_l^k\left[\Theta^{N-k+1}-\Theta^{N-k}\right] \tag{2}$$

where, $\Theta\left((N-k)\Delta\tau\right)$ is the excess temperature of a finite linear heat source per unit heat flux that starts to take effect at time $k\Delta\tau$ (the linear heat source is only distributed in the h_1-h_2 depth range) at any point A in the half-space, expressed as

$$\Theta^{N-k}=\Theta\left(\left(N-k\right)\Delta\tau\right)=\frac{1}{4\lambda\pi}\int_{h_1}^{h_2}\left\{\frac{erfc\left(\frac{\sqrt{r^2+\left(z-h\right)^2}}{2\sqrt{a\left(N-k\right)\Delta\tau}}\right)}{\sqrt{r^2+\left(z-h\right)^2}}-\frac{erfc\left(\frac{\sqrt{r^2+\left(z+h\right)^2}}{2\sqrt{a\left(N-k\right)\Delta\tau}}\right)}{\sqrt{r^2+\left(z+h\right)^2}}\right\}dh \tag{3}$$

According to the above analysis, an equal-time-interval heat flux series q_l^k acting from time $\tau=0$ is superimposed on the excess temperature $\theta^k(r,z,N\Delta\tau)$ generated by point A at time $N\Delta\tau$ to obtain an approximate solution of the excess temperature $\theta(r,z,N\Delta\tau)$ generated by $q_l(t)$ at point A, which can be expressed as

$$\theta\left(r,z,N\Delta\tau\right)=\sum_{k=1}^{N}\theta^{k}\left(r,z,N\Delta\tau\right)=\sum_{k=1}^{N}q_{l}^{k}\left[\Theta^{N-k+1}-\Theta^{N-k}\right] \tag{4}$$

3. Heat transfer model of W-tube buried-pipe energy pile considering heat exchange between circulating water and energy pile

3.1. Sectional superposition method for heat transfer of W - type buried energy pile

An energy pile is a new type of ground source heat pump system. Presently, common buried-pipe energy piles include the single U, double U, W, and spiral types. The W-type buried-pipe energy pile is shown in fig.3(a). Notably, it has many engineering applications due to its simple layout.

The buried depth of the pile top and pile bottom of the W-type buried-pipe energy pile, and the cylindrical coordinate system are established with a projection point O of the pile center on the ground being assumed as the coordinate origin. The positions of the four vertical heat exchange tubes of the W-type heat exchanger are (r_n, φ_n)（$n = 1\text{–}4$）

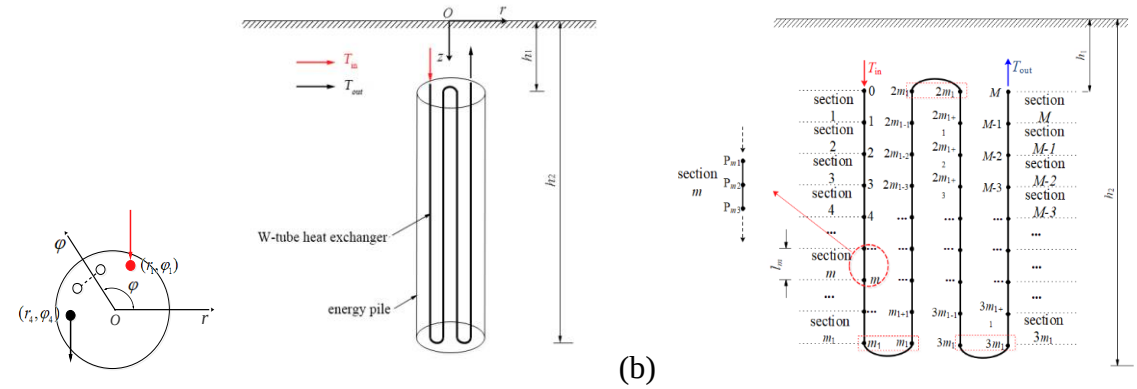

(a) (b)

Figure 3. (a) Illustration of a W- tube energy pile, (b) Section partition of a W-tube heat exchanger schematic diagram

When the circulating water flows, its temperature continuously decreases (or increases), and the heat exchange rate of the circulating water and the energy pile body vary at different positions of the heat exchange tube. The vertical buried-pipe section of a W-type heat exchanger can be divided into several sections to consider the difference in heat exchange efficiency between the circulating water and energy pile, and each vertical pipe is divided into m_1 sections, as shown in fig.3(b). Meanwhile, considering that the length of the adjacent vertical pipe connection section is much smaller than that of the vertical buried-pipe section, the heat exchange effect between the circulating water and energy pile in the connection section of the pipeline can usually be ignored. Accordingly, the heat transfer effect of the W-type heat exchanger can be regarded as the superposition of the heat transfer effect of each vertical section of the heat exchange tube, which is defined as the segmented superposition method.

To establish the piecewise superposition heat transfer model of a W-type buried-pipe energy pile, the following assumptions are made:

(1) The energy pile and soil around the pile are completely homogeneous mediums, and the physical parameters of the soil around the pile are used to simplify the calculation.

(2) Each section of the heat exchange tube can be regarded as a linear heat source of finite length, and the heat per unit length in this section is uniform.

(3) Without considering the heat transfer effect of the connecting section between adjacent vertical buried-pipe sections, the circulating water temperature is considered equal at both ends of the connecting section (as shown in the rectangular frame in fig.3(b)).

According to the segmentation shown in fig.3(b), for the m-segment of the heat exchange tube, h_{m1} is the initial depth of the segment, h_{m2} is the cut-off depth, and $l_m = h_{m2} - h_{m1}$ is the vertical segmentation length; the circulating water temperature at the starting point of the heat exchange tube is $T_{m\text{-}1}^{w}(\tau)$; and the circulating water temperature at the cutoff point is $T_m^w(\tau)$, where $T_0^w(\tau)$ is the inlet temperature T_{in}^w. The number of heat exchange tube nodes on both sides of the connecting section is the same, indicating that the circulating water temperature of the two points is the same, and the circulating water has no heat exchange effect during flow in the connecting section.

In addition, for the m-segment exchange tube, because the circulating water temperature and pile temperature outside the tube wall change with time, the unit length calorific value q_{lm} of the heat exchange tube is also a time-varying variable $q_{lm}(\tau)$, which is approximated using the method detailed in Section 2.2. The heat flux density in period $(k-1)\Delta\tau \sim k\Delta\tau$ can be expressed as q_{lm}^k.

According to Section 2.2, the excess temperature generated by the m-segment pile heat exchanger at $N\Delta\tau$ for any point A in the half space can be expressed as

$$\theta_m(r_{\text{A}}, \varphi_{\text{A}}, z_{\text{A}}, N\Delta\tau) = \sum_{k=1}^{N} \theta_m^k(r_{\text{A}}, \varphi_{\text{A}}, z_{\text{A}}, N\Delta\tau) = \sum_{k=1}^{N} q_{lm}^k \left[\Theta_{\text{A}}^{m,N-k+1} - \Theta_{\text{A}}^{m,N-k} \right] \tag{5}$$

Here, r_A, φ_A, and z_A are the cylindrical coordinates of any point A; $\Theta_A^{m,N-k}$ is the excess temperature generated by the unit-strength heat source of the m-segment pile foundation heat exchanger at $\tau = 0$ to any point A at time $(N-k)\Delta\tau$. According to Eq. (3), $\Theta_A^{m,N-k}$ can be expressed as

$$\Theta_A^{m,N-k} = \frac{1}{4\lambda\pi} \int_{h_{m1}}^{h_{m2}} \left\{ \frac{erfc\left(\dfrac{\sqrt{r_{Am}^2 + (z_A - h)^2}}{2\sqrt{a(N-k)\Delta\tau}} \right)}{\sqrt{r_{Am}^2 + (z_A - h)^2}} - \frac{erfc\left(\dfrac{\sqrt{r_{Am}^2 + (z_A + h)^2}}{2\sqrt{a(N-k)\Delta\tau}} \right)}{\sqrt{r_{Am}^2 + (z_A + h)^2}} \right\} \mathrm{d}h \tag{6}$$

$$r_{Am} = \sqrt{(r_A cos\varphi_A - r_m cos\varphi_m)^2 + (r_A sin\varphi_A - r_m sin\varphi_m)^2} \tag{7}$$

where r_{Am} is the projection distance between point A and the m-segment heat exchanger on the ground, and r_m and φ_m are the radial and axial-angle coordinates of the m-segment heat exchanger.

Because the pile foundation heat exchanger is divided into multiple segments, each segment will have an excess-temperature effect on any point A in space. Therefore, the excess temperature generated by the pile-foundation heat exchanger at point A can be regarded as the superposition of the excess temperature θ_m generated by each segment. Considering piecewise superposition, the excess temperature of any point A at time $N\Delta\tau$ can be expressed as

$$\theta(r_{\text{A}}, \varphi_{\text{A}}, z_{\text{A}}, N\Delta\tau) = \sum_{m=1}^{M} \theta_m(r_{\text{A}}, \varphi_{\text{A}}, z_{\text{A}}, N\Delta\tau) = \sum_{m=1}^{M} \sum_{k=1}^{N} q_{lm}^k \left[\Theta_{\text{A}}^{m,N-k+1} - \Theta_{\text{A}}^{m,N-k} \right] \tag{8}$$

where M is the total number of heat exchanger segments and $M = 4m_1$.

Eq. (8) is the piecewise superposition model for a variable heat source of a W-type buried-pipe energy pile. If the calorific value q_{lm}^k per unit length of each heat exchange tube at different times

can be solved, and the excess temperature response of any point in the half-space can be calculated according to the piecewise superposition in Eq. (8).

3.2. Single-pile piecewise superposition heat transfer model considering heat transfer effect of circulating water–energy pile

The underlying principle for establishing the piecewise superposition heat transfer model for a variable heat source of a single W-type buried-pipe energy pile involves solving the instantaneous heat generation per unit length of each heat exchange tube. The circulating water temperature in the heat exchange tube and the temperature outside the tube wall can be calculated using the thermal resistance method. Accordingly, this section will establish a single-pile variable-heat-source piecewise-superposition heat transfer model based on the piecewise superposition method of the energy-pile heat transfer considering the heat transfer effect of the circulating water-energy pile.

3.2.1 Excess temperature of the outer wall of the heat exchange tube for each heat-exchanger section

To simplify the calculation, it is assumed that the excess temperature of the outer wall of the heat exchange tube in the i-section at time $N\Delta\tau$ has a mean of $\theta_{\mathrm{b}i}(N\Delta\tau)$. The average value of the excess temperature of the outer wall of the heat exchange tube at different positions in this section can be taken as $\theta_{\mathrm{b}i}(N\Delta\tau)$, and the average value of the excess temperature from p_{i1} to p_{i3} (the first, middle, and last three points of the i-section) can be approximated as follows:

$$\theta_{\mathrm{b}i}(N\Delta\tau)=\frac{1}{3}\sum_{j=1}^{3}\theta_{\mathrm{b}i,j}(N\Delta\tau) \tag{9}$$

In Eq. (9), $\theta_{\mathrm{b}i,j}(N\Delta\tau)$ is the excess temperature at point p_{ij} on the outer wall of the heat exchange tube in the i-section at time $N\Delta\tau$.

In the segmented superposition method, the average excess temperature $N\Delta\tau$ of the outer wall of the heat exchange tube at the i-section at time $\theta_{\mathrm{b}i,j}(N\Delta\tau)$ can be regarded as a superposition of the excess outer wall temperature of the i-section heat exchanger produced by each segment heat exchanger:

$$\theta_{\mathrm{b}i}(N\Delta\tau)=\sum_{m=1}^{M}\theta_{\mathrm{b}i}^{m}(N\Delta\tau) \tag{10}$$

In Eq. (10), $\theta_{\mathrm{b}i}^{m}(N\Delta\tau)$ is the average excess temperature of the outer wall of the heat exchange tube of the i-section heat exchanger caused by the section m heat exchanger at time $N\Delta\tau$.

According to Eqs. (9) and (10), and referring to Eq. (8), the following can be derived:

$$\theta_{\mathrm{b}i}^{N}=\theta_{\mathrm{b}i}(N\Delta\tau)=\frac{1}{3}\sum_{j=1}^{3}\sum_{m=1}^{M}\sum_{k=1}^{N}q_{lm}^{k}\left[\Theta_{i,j}^{m,N-k+1}-\Theta_{i,j}^{m,N-k}\right] \tag{11}$$

In Eq. (11), $\Theta_{i,j}^{m,N-k}$ is the excess temperature generated by the unit-strength heat source acting on the outer wall at point p_{ij} of the heat exchange tube of the i-segment heat exchanger at instant $(N-k)\Delta\tau$ from the m-segment heat exchanger at instant $\tau=0$.

3.2.2 Heat exchange between circulating water and outer wall of heat exchange tube

According to heat conduction theory, the heat transfer between the circulating water in the heat exchange tube and outer wall of the tube at $N\Delta\tau$ can be expressed as follows:

$$q_{lm}^{N}=\frac{\overline{T}_{m}^{\mathrm{w}N}-T_{m}^{\mathrm{b}N}}{R_{\mathrm{p}}} \tag{12}$$

$$\overline{T}_{\mathrm{m}}^{\mathrm{w}N}=\frac{T_{\mathrm{m\text{-}1}}^{\mathrm{w}N}+T_{\mathrm{m}}^{\mathrm{w}N}}{2} \tag{13}$$

$$T_{m}^{\mathrm{b}N}=\theta_{\mathrm{b}m}^{N}+T_{0} \tag{14}$$

where $\bar{T}_{m}^{wN}$ is the average temperature of the circulating water in the m-section heat exchange tube at $N\Delta\tau$; $T_{m\text{-}1}^{wN}$ and T_{m}^{wN} are the temperatures of the circulating water at node m - 1 and m at $N\Delta\tau$; $T_{m}^{\mathrm{b}N}$ is the average temperature of the outer wall of the m-segment heat exchange tube at $N\Delta\tau$; T_0 is the initial temperature; and R_p is the heat transfer resistance between the circulating water and outer wall of the heat exchange tube, which can be expressed as

$$R_{\mathrm{p}}=\frac{1}{2\pi\lambda_{\mathrm{p}}}\ln\frac{r_{\mathrm{o}}^{\mathrm{p}}}{r_{\mathrm{i}}^{\mathrm{p}}}+\frac{1}{2\pi r_{\mathrm{i}}^{\mathrm{p}}h_{\mathrm{f}}} \tag{15}$$

$$h_{\mathrm{f}}=\frac{\lambda_{\mathrm{f}}\times N_{\mathrm{u}}}{2r_{\mathrm{i}}^{\mathrm{p}}} \tag{16}$$

where λ_{p} and λ_{f} are the thermal conductivity （$\mathrm{W\cdot m^{-1}\cdot K^{-1}}$） of the tube wall and circulating water, respectively, and $r_{\mathrm{i}}^{\mathrm{p}}$ and $r_{\mathrm{o}}^{\mathrm{p}}$ are the inner (m) and outer wall radii (m) of the heat exchange tube, respectively. N_{u} should be defined as the Nusselt number and its value given as it is a constant for laminar flow in circular tubes.

3.2.3 Energy loss in circulating water in the heat exchanger

At instant $N\Delta\tau$, the circulating water temperature at the starting node of the m-segment heat exchanger is $T_{m\text{-}1}^{wN}$, and the temperature of the circulating water at the cut-off point is T_{m}^{wN}. The energy loss in the circulating water in the segment heat exchanger is

$$T_{m-1}^{\mathrm{w}N}\text{-}T_{m}^{\mathrm{w}N}=\frac{q_{lm}^{N}l_{m}}{c_{\mathrm{f}}m_{\mathrm{f}}} \tag{17}$$

where c_{f} and m_{f} are the specific heat capacity（$\mathrm{J\cdot kg^{-1}\cdot K^{-1}}$）and mass flow rate（$\mathrm{kg\cdot s^{-1}}$）of the circulating water, respectively, whereas the other parameters are maintained constant.

3.2.4 Segmented heat flux-water temperature equations of single energy pile

The heat flux q_{lm}^{k} in each segment of the heat exchanger can be calculated through three processes, namely, heat transfer inside the circulating water in the heat exchanger, heat transfer between the circulating water and the outer wall of the heat exchange tube, and heat transfer between the heat exchange tube and energy pile (or surrounding rock and soil).

The piecewise superposition method considers the contribution of each section of the heat exchanger, the heat transfer between the circulating water in each section, and the heat exchange tube, and the energy pile is combined to obtain the piecewise heat flux–water temperature equation set of the W-type buried energy pile at $N\Delta\tau$:

$$\mathbf{A}\mathbf{X}^{NT}=\mathbf{B}\quad(N=1,2,3.....) \tag{18}$$

$$\mathbf{X}^{NT}=[q_{l1}^{N}\quad q_{l2}^{N}\quad\cdots\quad q_{lM}^{N}\quad T_{1}^{wN}\quad T_{2}^{wN}\quad\cdots\quad T_{M}^{wN}]^{T} \tag{19}$$

$$\mathbf{B}=\begin{Bmatrix} \frac{1}{2}T_{\text{in}}^{N}-T_0-\frac{1}{3}\sum_{m=1}^{M}\sum_{k=1}^{N-1}q_{lm}^{k}\left[\sum_{j=1}^{3}\Theta_{1,j}^{m,N-k+1}-\sum_{j=1}^{3}\Theta_{1,j}^{m,N-k}\right] \\ -T_0-\frac{1}{3}\sum_{m=1}^{M}\sum_{k=1}^{N-1}q_{lm}^{k}\left[\sum_{j=1}^{3}\Theta_{2,j}^{m,N-k+1}-\sum_{j=1}^{3}\Theta_{2,j}^{m,N-k}\right] \\ \cdots \\ -T_0-\frac{1}{3}\sum_{m=1}^{M}\sum_{k=1}^{N-1}q_{lm}^{k}\left[\sum_{j=1}^{3}\Theta_{M,j}^{m,N-k+1}-\sum_{j=1}^{3}\Theta_{M,j}^{m,N-k}\right] \\ -T_{\text{in}}^{N} \\ 0 \\ \cdots \\ 0 \end{Bmatrix} \tag{20}$$

$$\mathbf{A}=\begin{bmatrix} \mathbf{A}_{11} & \mathbf{A}_{12} \\ \mathbf{A}_{21} & \mathbf{A}_{22} \end{bmatrix} \tag{21}$$

where $\mathbf{A}_{11}$, $\mathbf{A}_{12}$, $\mathbf{A}_{21}$, and $\mathbf{A}_{22}$ are submatrices of the coefficient matrix, expressed as follows:

$$\mathbf{A}_{11}=\begin{bmatrix} R_{\text{p}}+\frac{1}{3}\sum_{j=1}^{3}\Theta_{1,j}^{1,1} & \frac{1}{3}\sum_{j=1}^{3}\Theta_{1,j}^{2,1} & \cdots & \frac{1}{3}\sum_{j=1}^{3}\Theta_{1,j}^{M,1} \\ \frac{1}{3}\sum_{j=1}^{3}\Theta_{2,j}^{1,1} & R_{\text{p}}+\frac{1}{3}\sum_{j=1}^{3}\Theta_{2,j}^{2,1} & \cdots & \frac{1}{3}\sum_{j=1}^{3}\Theta_{2,j}^{M,1} \\ \cdots & \cdots & \cdots & \cdots \\ \frac{1}{3}\sum_{j=1}^{3}\Theta_{M,j}^{1,1} & \frac{1}{3}\sum_{j=1}^{3}\Theta_{M,j}^{2,1} & \cdots & R_{\text{p}}+\frac{1}{3}\sum_{j=1}^{3}\Theta_{M,j}^{M,1} \end{bmatrix} \tag{22}$$

$$\mathbf{A}_{12}=\begin{bmatrix} -0.5 & 0 & 0 & \cdots & 0 \\ -0.5 & -0.5 & 0 & \cdots & 0 \\ 0 & -0.5 & -0.5 & \cdots & 0 \\ \cdots & \cdots & \cdots & \cdots & \cdots \\ 0 & \cdots & 0 & -0.5 & -0.5 \end{bmatrix} \tag{23}$$

$$\mathbf{A}_{21}=\begin{bmatrix} -\frac{l_1}{c_{\text{f}}m_{\text{f}}} & 0 & 0 & \cdots & 0 \\ 0 & -\frac{l_2}{c_{\text{f}}m_{\text{f}}} & 0 & \cdots & 0 \\ 0 & 0 & -\frac{l_3}{c_{\text{f}}m_{\text{f}}} & \cdots & 0 \\ \cdots & \cdots & \cdots & \cdots & \cdots \\ 0 & 0 & 0 & \cdots & -\frac{l_{\text{M}}}{c_{\text{f}}m_{\text{f}}} \end{bmatrix} \tag{24}$$

$$\mathbf{A}_{22}=\begin{bmatrix} -1 & 0 & 0 & \cdots & 0 \\ 1 & -1 & 0 & \cdots & 0 \\ 0 & 1 & -1 & \cdots & 0 \\ \cdots & \cdots & \cdots & \cdots & \cdots \\ 0 & \cdots & 0 & 1 & -1 \end{bmatrix} \tag{25}$$

By solving the above equations, the heat flux q_{lm}^{N} generated by each section of the W-type buried-pipe energy pile at $N\Delta\tau$ and the circulating water temperature T_m^{WN} in the heat exchange tube can be obtained.

The calculation is sequentially conducted from $1\Delta\tau$ until $N\Delta\tau$ to obtain the heat flux q_{lm}^{k}（$k=1\sim N$ generated by the heat exchanger in each section during period $1\Delta\tau\sim N\Delta\tau$. Substituting the heat flux density q_{lm}^{k} generated in each segment of the heat exchanger at $1\Delta\tau-N\Delta\tau$ period into Eq. (10) yields the excess temperature of any point A in the half-space at instance $N\Delta\tau$, which is the segmented superposition heat-transfer model for a W-type buried-pipe energy pile with a variable heat source.

4. Model validation

To ensure the correctness of the heat transfer model of the W-type buried-pipe energy pile, the Bezyan numerical model in [22] and the calculation results of the proposed model are verified using FLUENT software and MATLAB, respectively. Because the pile and soil parameters in Bezyan 's numerical model differ, the soil parameters are taken as the pile–soil parameters. The soil temperatures perpendicular to the side of the intake pipe at underground depths of 10 m and 25 m were compared. The model parameters are listed in tab.1.

Table 1. Parameters of the model

parameter		parameter	
Pile–soil thermal conductivity/W·m^{-1}·K^{-1}	1.3	Pile-soil density/kg·m^{-3}	1847
Pile-soil heat capacity/J·kg^{-1}·K^{-1}	1200	The mass flow rate of water /kg·s^{-1}	0.095
Inlet temperature/℃	35	Initial temperature/℃	18.2
Heat exchanger length/m	20	Heat exchanger spacing/m	0.6
Tube inner diameter/mm	20	Tube outer diameter/mm	24
Pile top depth/m	5	Pile bottom depth/m	25
Tube thermal conductivity/W·m^{-1}·K^{-1}	0.42		

Figure 4 shows the comparison of the soil temperature of the two models on the side of the inlet pipe at different depths. For a certain point in the soil, the temperature change trend obtained using the two methods is the same, and the absolute error does not exceed 0.2 °C. Therefore, the proposed new model considering the heat exchange effect of circulating water-energy pile is reliable.

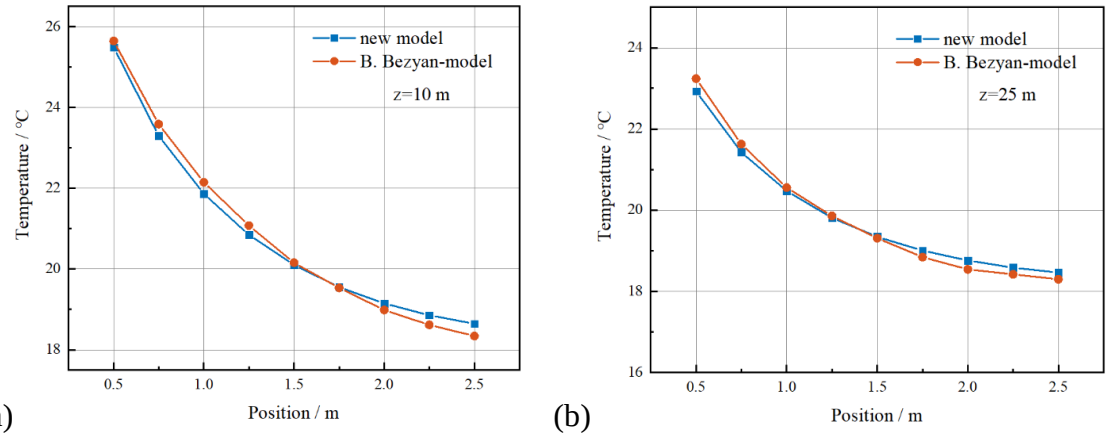

Figure 4. The soil temperature of the two models on the side of the inlet pipe at different depths; (a) *z*=10m and (b) *z*=25m

5. Results and Analysis

5.1. Change of water temperature in heat exchanger

In this section, the calculation of circulating fluid temperatures at various locations within the heat exchanger is undertaken to enhance the representation of heat transfer characteristics associated with the W-type buried energy pile. The parameters employed for this analysis remain consistent with those presented in tab. 1. The outcomes are graphically presented in fig. 5. Notably, the temperature alteration is more pronounced in proximity to the outlet, while it is comparatively subdued near the inlet. Additionally, as time elapses, the extent of temperature variation progressively diminishes.

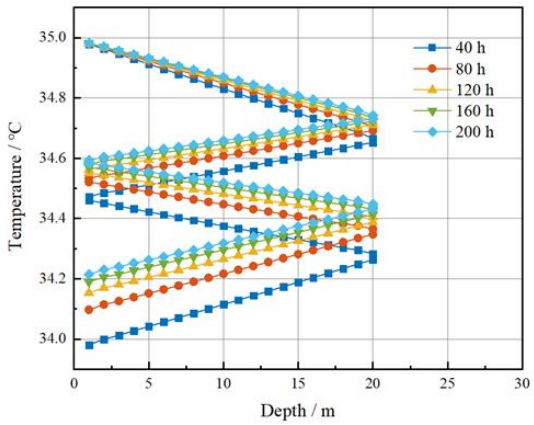

Figure 5. Change of water temperature in heat exchanger

5.2. Change of heat flow density in the heat exchanger

In this section, an analysis is conducted to ascertain the heat transfer characteristics of the W-type buried energy pile, with a focus on determining the heat flux density variations at distinct positions along the heat exchanger. The parameters utilized for the calculations remain consistent with those outlined in tab. 1. Figure 6 presents the obtained results. Notably, the graph illustrates a significant decline in heat flux density over time. The highest heat flux density is observed at the inlet, while the first and fourth sections of the heat exchanger exhibit greater heat flux density compared to

the second and third sections. Moreover, the heat flux density at the upper and lower extremities is greater than the heat flux of the rest of the segment.

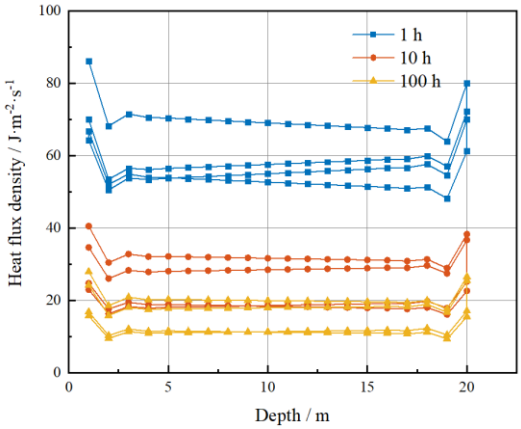

Figure 6. Change of heat flow density in heat exchanger

5.3. Heat exchange analysis of different mass flow rate

In this section, mass flow rates of 0.05 kg·s^{-1}, 0.1 kg·s^{-1}, 0.15 kg·s^{-1}, and 0.2 kg·s^{-1} are considered while the other parameters remain unchanged (see tab. 1.). The heat exchange per meter and total heat exchange after heat exchange in the energy piles at the aforementioned mass flow rates are analyzed, and the results are shown in fig. 7. The heat transfer per meter increases with the mass flow rate, and the heat transfer efficiency is significantly improved between 0.05 kg·s^{-1} and 0.15 kg·s^{-1}. When the mass flow rate is greater than 0.15 kg·s^{-1}, the heat transfer per meter is slightly increased. Therefore, improving the mass flow rate of the circulating water can improve the heat transfer efficiency of the energy pile, and the optimal mass flow rate range is between 0.05 kg·s^{-1} and 0.15 kg·s^{-1}.

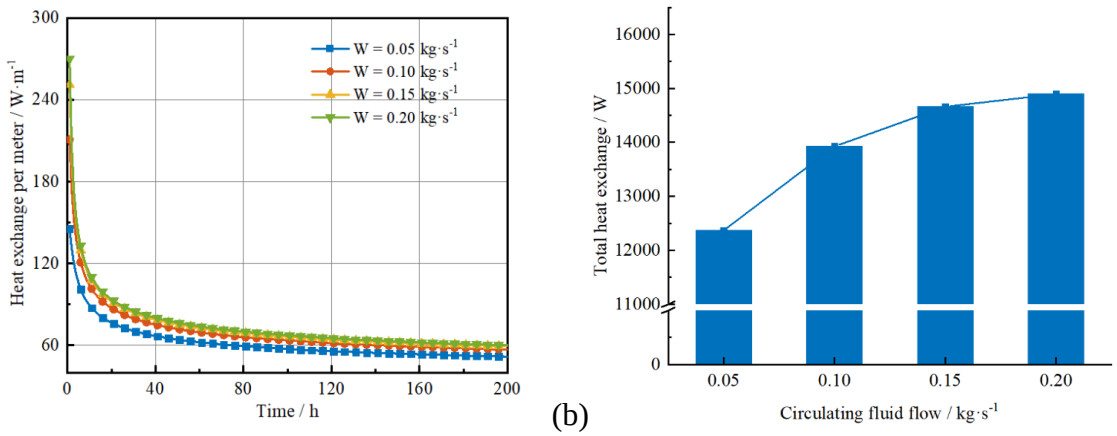

(a) (b)

Figure 7. Heat exchange at different mass flow rates; (a) Heat exchange per meter, and(b) Total heat exchange

5.4. Heat exchange analysis of different thermal conductivity

In this section, pile–soil thermal conductivities of 1 W·m^{-1}·K^{-1}, 2 W·m^{-1}·K^{-1}, 3 W·m^{-1}·K^{-1}, and 4 W·m^{-1}·K^{-1} are compared, whereas the other parameters remain unchanged (see tab. 1.). This section analyzes the heat exchange per meter for energy piles with four pile–soil thermal conductivities, and the results are shown in fig. 8. When the pile–soil thermal conductivity increases from 1 W·m^{-1}·K^{-1} to

2 $W \cdot m^{-1} \cdot K^{-1}$, 3 $W \cdot m^{-1} \cdot K^{-1}$, and 4 $W \cdot m^{-1} \cdot K^{-1}$, the heat transfer efficiency of the energy pile increases by 61%, 110% and 153%, respectively. Therefore, improving the pile–soil thermal conductivity is an effective method of improving the heat transfer efficiency of the energy pile.

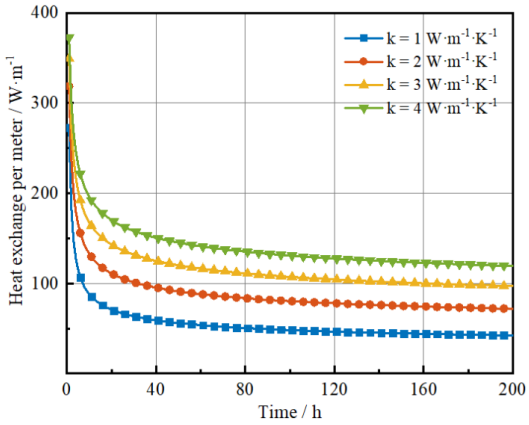

Figure 8. Heat exchange per meter for different pile–soil thermal conductivities

5.5. Heat exchange analysis for different densities

In this section, pile and soil densities of 1600 $kg \cdot m^{-3}$, 1900 $kg \cdot m^{-3}$, 2200 $kg \cdot m^{-3,}$ and 2500 $kg \cdot m^{-3}$ were considered, whereas other parameters remained unchanged (tab. 1.). This section analyzes the heat exchange per meter of the energy pile under the four density conditions, and the results are shown in fig. 9. The heat exchange per meter increases with an increase in density due to the greater density decreasing the thermal diffusivity, the difficulty of increasing the concrete temperature, the large difference between the concrete and pipe water temperature, and the high rate of heat transfer.

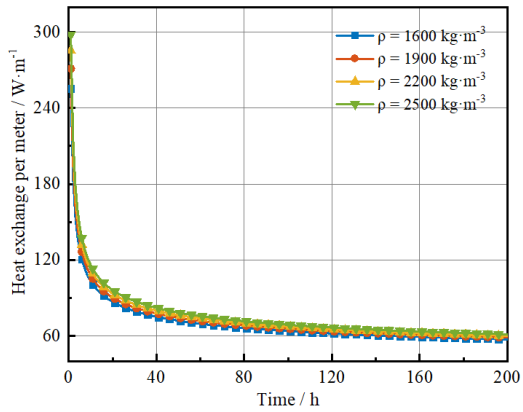

Figure 9. Heat exchange per meter for different pile–soil densities

5.6. Heat exchange analysis of different specific heat capacity

In this section, the specific heat capacity of the pile–soil is 737 $J \cdot kg \cdot K^{-1}$, 837 $J \cdot kg \cdot K^{-1}$, 937 $J \cdot kg \cdot K^{-1}$, and 1037 $J \cdot kg \cdot K^{-1}$, whereas the other parameters are maintained constant (see tab. 1.). This section analyzes the heat transfer per meter of the energy pile under the four specific heat capacities, and the results are shown in fig. 10. The heat transfer per meter increases with the increase in specific heat capacity. Similar to the density, the large specific heat capacity is due to the greater density

decreasing the thermal diffusivity, the difficulty of increasing the concrete temperature, the large difference between the concrete and pipe water temperature, and the high rate of heat transfer.

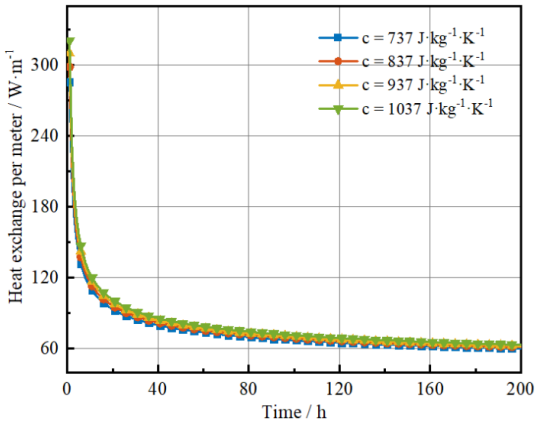

Figure 10. Heat exchange per meter for different pile–soil specific heat capacities

6. Conclusion

To better describe the actual heat transfer process of energy pile, this paper establishes the heat transfer model of W-type buried-pipe energy pile under the condition of variable heat source.

(1) In this study, each heat exchange tube in a W-type heat exchanger is regarded as a finite linear heat source. Under a variable heat flow and applying the Green function theory and piecewise superposition method based on the heat transfer model of an energy pile, the heat transfer model of a single W-type energy pile, considering the heat exchange between the circulating water and energy pile, is obtained. This model can assist in obtaining a time-varying heat flux and a precise exit temperature, which is useful for quickly assessing the heat exchange efficiency of the energy pile.

(2) This model is compared with the soil temperature in the literature obtained from a FLUENT numerical model. Compared with the numerical model, the absolute error between them is less than 0.2 ℃, validating the accuracy of the single-pile variable-heat-source model of the W-type energy pile established in this study.

(3) In order to better reflect the heat transfer characteristics of the W-type buried energy pile, this article analyzes the changes in water temperature and heat flux density at different positions of the heat exchanger. The water temperature inside the W-type heat exchanger also shows a W-shaped variation. The temperature change is larger on the side closer to the outlet and smaller on the side closer to the inlet. Moreover, as time increases, the temperature change gradually decreases. The heat flux density decreases significantly with time. The highest heat flux density is observed at the inlet, while the first and fourth sections of the heat exchanger exhibit greater heat flux density compared to the second and third sections. Moreover, the heat flux density at the upper and lower extremities is greater than the heat flux of the rest of the segment.

(4) The heat transfer analysis of the W-type tubular energy pile was conducted using a heat transfer model to account for variations in the mass flow rate, pile–soil thermal conductivity, pile–soil density, and pile–soil specific heat capacity. The heat transfer per meter increases with an increase in the mass flow rate, and the optimal mass flow rate is between 0.05 $kg \cdot s^{-1}$ and 0.15 $kg \cdot s^{-1}$. When the pile–soil thermal conductivity increases from 1 $W \cdot m^{-1} \cdot K^{-1}$ to 2, 3, and 4 $W \cdot m^{-1} \cdot K^{-1}$, the heat transfer

efficiency of the energy pile increases by 61%, 110%, and 153%, respectively. Thus, improving the pile–soil thermal conductivity is an effective method of improving the heat transfer efficiency of energy piles. Heat transfer per meter increases with the increase in density and specific heat capacity.

Acknowledgments

We would like to thank KetengEdit (www.ketengedit.com) for its linguistic assistance during the preparation of this manuscript.

References

[1] Xie, J., Qin, Y., Heat transfer and bearing characteristics of energy piles: Review, *Energies*, 14(2021), 20, pp. 6483.
[2] Quaggiotto., *et al.*, Simulation-Based comparison between the thermal behavior of coaxial and double U-Tube borehole heat exchangers, *Energies*, 12(2019), 12, pp. 2321.
[3] Wang, J., *et al.*, Performance investigation of a new geothermal combined cooling, heating and power system, *Energy Conversion and Management*, 208(2020), pp. 112591.
[4] Florides, G., Kalogirou, S., Ground heat exchangers—a review of systems, models and applications, *Renewable Energy*, 32(2007), 15, pp. 2461-2478.
[5] Li, M., Lai, A. C. K., Review of analytical models for heat transfer by vertical ground heat exchangers (GHEs): A perspective of time and space scales, *Applied Energy*, 151(2015), pp. 178-191.
[6] Yang, H., *et al.*, Vertical-borehole ground-coupled heat pumps: A review of models and systems, *Applied Energy*, 87(2010), 1, pp. 16-27.
[7] Cui, Y., *et al.*, A comprehensive review on 2D and 3D models of vertical ground heat exchangers, *Renewable and Sustainable Energy Reviews*, 94(2018), pp. 84-114.
[8] Plass, L. I. H., Theory of the ground pipe heat source for the heat pump, *ASHVE Transactions*, 20(1948), 7, pp. 119-122.
[9] Zeng, H. Y., *et al.*, A finite line-source model for boreholes in geothermal heat exchangers, *Heat Transfer-Asian Research*, 31(2002), 7, pp. 558-567.
[10] Kavanaugh, S. P., Simulation and experimental verification of vertical ground-coupled heat pump systems, Oklahoma State University, Oklahoma, 1985.
[11] Man, Y., *et al.*, A new model and analytical solutions for borehole and pile ground heat exchangers, *International Journal of Heat and Mass Transfer*, 53(2010), 13-14, pp. 2593-2601.
[12] Man, Y. Y. H. D., Development of spiral heat source model for novel pile ground heat exchangers, *HVAC&R research*, 17(2011), 6.
[13] Cui, P., *et al.*, Heat transfer analysis of pile geothermal heat exchangers with spiral coils, *Applied Energy*, 88(2011), 11, pp. 4113-4119.
[14] Yang,W., Shi,M., Study on heat transfer model of vertical U-tube ground heat exchangers based on line heat source theory, *Acta Energiae Solaris Sinica*, 05(2007), pp. 482-488.
[15] Ang,C., *et al.*, Heat transfer model of ground heat exchanger under variable heat flux and its experimental verification, *Refrigeration and Air-Conditioning*, 14(2014), 02, pp. 41-44.
[16] Akrouch, G. A., *et al.*, An experimental, analytical and numerical study on the thermal efficiency of energy piles in unsaturated soils, *Computers and Geotechnics*, 71(2016), pp. 207-220.
[17] Li, M., Lai, A. C. K., Analytical model for short-time responses of ground heat exchangers with

U-shaped tubes: Model development and validation, *Applied Energy*, 104(2013), pp. 510-516.
[18] Li, M., Lai, A. C. K., New temperature response functions (G functions) for pile and borehole ground heat exchangers based on composite-medium line-source theory, *Energy*, 38(2012), 1, pp. 255-263.
[19] Li, M., Lai, A. C. K., Heat-source solutions to heat conduction in anisotropic media with application to pile and borehole ground heat exchangers, *Applied Energy*, 96(2012), pp. 451-458.
[20] Luo, Y., *et al.*, Integrated analytical modeling of transient heat transfer inside and outside U-tube ground heat exchanger: A new angle from composite-medium method, *International Journal of Heat and Mass Transfer*, 162(2020), pp. 120373.
[21] You, T., *et al.*, Soil thermal imbalance of ground source heat pump systems with spiral-coil energy pile groups under seepage conditions and various influential factors, *Energy Conversion and Management*, 178(2018), pp. 123-136.
[22] Bezyan, B., *et al.*, 3-D simulation of heat transfer rate in geothermal pile-foundation heat exchangers with spiral pipe configuration, *Applied Thermal Engineering*, 87(2015), pp. 655-668.

Paper submitted: 03.06.2023
Paper revised: 10.07.2023
Paper accepted: 18.07.2023